Measurements of polarimetric sensitivity to hydrostatic pressure, strain and temperature in birefringent dual-core microstructured polymer fiber

Marcin K. Szczurowski,[1] Tadeusz Martynkien,[1] Gabriela Statkiewicz-Barabach, [1]Waclaw Urbanczyk,[1,*] and David J. Webb[2]

[1]Institute of Physics, Wroclaw University of Technology, Wybrzeze Wyspianskiego 27, 50-370 Wroclaw, Poland
[2]Photonics Research Group, Aston University, Birmingham, B4 7ET, UK
**waclaw.urbanczyk@pwr.wroc.pl*

Abstract: We experimentally characterized a birefringent microstructured polymer fiber of specific construction, which allows for single mode propagation in two cores separated by a pair of large holes. The fiber exhibits high birefringence in each of the cores as well as relatively weak coupling between the cores. Spectral dependence of the group and the phase modal birefringence was measured using an interferometric method. We have also measured the sensing characteristics of the fiber such as polarimetric sensitivity to hydrostatic pressure, strain and temperature. Moreover, we have studied the effect of hydrostatic pressure and strain on coupling between the cores.

OCIS codes: (060.2310) Fiber optics; (060.2370) Fiber optics sensors; (060.2270) Fiber characterization; (060.4005) Microstructured fibers; (160.5470) Polymers.

References and links:

1. P. St. J. Russell, "Photonic crystal fibers," Science **299**(5605), 358–362 (2003).
2. T. M. Monro, W. Belardi, K. Furusawa, J. C. Baggett, N. G. R. Broderick, and D. J. Richardson, "Sensing with microstructured optical fibres," Meas. Sci. Technol. **12**(7), 854–858 (2001).
3. J. M. Fini, "Microstructure fibres for optical sensing in gases and liquids," Meas. Sci. Technol. **15**(6), 1120–1128 (2004).
4. G. Statkiewicz, T. Martynkien, and W. Urbanczyk, "Measurements of modal birefringence and polarymetic sensitivity of the birefringent holey fiber to hydrostatic pressure and strain," Opt. Commun. **241**(4-6), 339–348 (2004).
5. C. M. B. Cordeiro, M. A. R. Franco, G. Chesini, E. C. S. Barretto, R. Lwin, C. H. Brito Cruz, and M. C. J. Large, "Microstructured-core optical fibre for evanescent sensing applications," Opt. Express **14**(26), 13056–13066 (2006).
6. O. Frazão, J. L. Santos, F. M. Araujo, and L. A. Ferreira, "Optical sensing with photonic crystal fibers," Laser Photonics Rev. **2**(6), 449–459 (2008).
7. S. Kiesel, K. Peters, T. Hassan, and M. Kowalsky, "Large deformation in-fiber polymer optical fiber sensor," IEEE Photon. Technol. Lett. **20**(6), 416–418 (2008).
8. S. Kiesel, K. Peters, T. Hassan, and M. Kowalsky, "Behaviour of intrinsic polymer optical fibre sensor for large-strain applications," Meas. Sci. Technol. **18**(10), 3144–3154 (2007).
9. M. Silva-López, A. Fender, W. N. MacPherson, J. S. Barton, J. D. C. Jones, D. Zhao, H. Dobb, D. J. Webb, L. Zhang, and I. Bennion, "Strain and temperature sensitivity of a single-mode polymer optical fiber," Opt. Lett. **30**(23), 3129–3131 (2005).
10. S. Muto, O. Suzuki, T. Amano, and M. Morisawa, "A plastic optical fibre sensor for real-time humidity monitoring," Meas. Sci. Technol. **14**(6), 746–750 (2003).
11. X. H. Yang, and L. L. Wang, "Fluorescence pH probe based on microstructured polymer optical fiber," Opt. Express **15**(25), 16478–16483 (2007).
12. Z. Xiong, G. D. Peng, B. Wu, and P. L. Chu, "Highly tunable Bragg gratings in single-mode polymer optical fibers," IEEE Photon. Technol. Lett. **11**(3), 352–354 (1999).
13. K. E. Carroll, C. Zhang, D. J. Webb, K. Kalli, A. Argyros, and M. C. J. Large, "Thermal response of Bragg gratings in PMMA microstructured optical fibers," Opt. Express **15**(14), 8844–8850 (2007).
14. H. B. Liu, H. Y. Liu, G. D. Peng, and P. L. Chu, "Strain and temperature sensor using a combination of polymer,and silica fibre bragg gratings," Opt. Commun. **219**(1-6), 139–142 (2003).

#125168 - $15.00 USD Received 8 Mar 2010; revised 5 May 2010; accepted 5 May 2010; published 24 May 2010

15. M. A. van Eijkelenborg, M. C. J. Large, A. Argyros, J. Zagari, S. Manos, N. A. Issa, I. Bassett, S. Fleming, R. C. McPhedran, C. M. de Sterke, and N. A. P. Nicorovici, "Microstructured polymer optical fibre," Opt. Express **9**(7), 319–327 (2001).
16. G. Barton, M. A. van Eijkelenborg, G. Henry, M. C. J. Large, and J. Zagari, "Fabrication of microstructured polymer optical fibres," Opt. Fiber Technol. **10**(4), 325–335 (2004).
17. A. Argyros, I. Bassett, M. van Eijkelenborg, M. Large, J. Zagari, N. A. Nicorovici, R. McPhedran, and C. M. de Sterke, "Ring structures in microstructured polymer optical fibres," Opt. Express **9**(13), 813–820 (2001).
18. W. E. P. Padden, M. A. van Eijkelenborg, A. Argyros, and N. A. Issa, "Coupling in a twin-core microstructured polymer optical fiber," Appl. Phys. Lett. **84**(10), 1689–1691 (2004).
19. X. Yu, M. A. van Eijkelenborg, and P. Shum, "Determination of the wavelength dependence of the coupling effect in twin-core microstructured polymer optical fibers," Opt. Eng. **46**(7), 075002 (2007).
20. Y. Zhang, L. Ren, K. Li, H. Wang, W. Zhao, L. Wang, R. Miao, M. C. J. Large, and M. A. van Eijkelenborg, "Guiding mode in elliptical core microstructured polymer optical fiber," Chin. Opt. Lett. **5**, 194–196 (2007).
21. N. A. Issa, M. A. van Eijkelenborg, M. Fellew, F. Cox, G. Henry, and M. C. J. Large, "Fabrication and study of microstructured optical fibers with elliptical holes," Opt. Lett. **29**(12), 1336–1338 (2004).
22. A. Argyros, M. A. van Eijkelenborg, M. C. Large, and I. M. Bassett, "Hollow-core microstructured polymer optical fiber," Opt. Lett. **31**(2), 172–174 (2006).
23. H. Dobb, D. J. Webb, K. Kalli, A. Argyros, M. C. J. Large, and M. A. van Eijkelenborg, "Continuous wave ultraviolet light-induced fiber Bragg gratings in few- and single-mode microstructured polymer optical fibers," Opt. Lett. **30**(24), 3296–3298 (2005).
24. M. A. van Eijkelenborg, W. Padden, and J. A. Besley, "Mechanically induced long-period gratings in microstructured polymer fibre," Opt. Commun. **236**(1-3), 75–78 (2004).
25. L. Zhang, C. Yang, C. Yu, T. Luo, and A. E. Willner, "PCF-based polarization splitters with simplified structures," J. Lightwave Technol. **23**(11), 3558–3565 (2005).
26. P. Hlubina, T. Martynkien, and W. Urbańczyk, "Dispersion of group and phase modal birefringence in elliptical-core fiber measured by white-light spectral interferometry," Opt. Express **11**(22), 2793–2798 (2003).
27. M. Szpulak, T. Martynkien, and W. Urbanczyk, "Effects of hydrostatic pressure on phase and group modal birefringence in microstructured holey fibers," Appl. Opt. **43**(24), 4739–4744 (2004).
28. M. Szpulak, T. Martynkien, and W. Urbańczyk, **"**Highly birefringent photonic crystal fibre with enhanced sensitivity to hydrostatic pressure,"in Proceedings of 2006 8th International Conference on Transparent Optical Networks with 5th European Symposium on Photonic Crystals (Nottingham, UK, June 18–22, 2006) Vol. **4 /** [Ed. M. Marciniak]. Piscataway, NJ: IEEE, cop. 2006, pp. 174–177.
29. W. Primak, and D. Post, "Photoelastic constants of vitreous silica and its elastic coefficient of refractive index," J. Appl. Phys. **30**(5), 779–788 (1959).
30. R. M. Waxler, D. Horowitz, and A. Feldman, "Optical and physical parameters of Plexiglas 55 and Lexan," Appl. Opt. **18**(1), 101–104 (1979).
31. S. Y. Huang, J. N. Blake, and B. Y. Kim, "Perturbation effects on mode propagation in highly elliptical core two-mode fibers," J. Lightwave Technol. **8**(1), 23–33 (1990).
32. W. Xu, X. F. Yao, H. Y. Yeh, and G. C. Jin, "Fracture investigation of PMMA specimen using coherent gradient sensing (CGS) technology," Polym. Test. **24**(7), 900–908 (2005).

1. Introduction

Photonic crystal fibers (PCFs) made of silica have been the subject of extensive research for over a decade [1]. It has been already demonstrated that silica PCFs can be used in numerous applications such as the generation of supercontinuum, compensation of chromatic dispersion, improvement in efficiency of fiber-optic lasers, and many others. There is also an increasing interest concerning metrological applications of silica PCFs [2–6], involving interferometric and polarimetric sensors of different physical parameters as well as evanescent field sensors for monitoring specific chemical compounds in gases and liquids [3,5].

In the last few years, interest in sensing applications of conventional polymer optical fibers (POFs) significantly increased. It is driven by the fact that POF possesses several advantages compared to silica fiber. In particular, POF is biocompatible, offers greater numerical aperture, more flexibility (lower Young's modulus) and can be exposed to much greater strain compared to silica. For these reasons, conventional POF has been already studied in numerous sensing applications including measurements of large strains [7–9], humidity [10], and pH [11]. The inscription of Bragg gratings in POF, first demonstrated in [12], opens now new sensing possibilities [13,14].

In the last decade the fabrication technology of microstructured polymer optical fibers (mPOFs) was mastered by several groups and mPOF of many different types has been reported in the literature. This new class of fibers combines the interesting physical and chemical properties of PMMA with the wide engineering freedom of microstructured fibers. The first single mode mPOF of hexagonal symmetry was demonstrated in [15]. As mPOF

#125168 - $15.00 USD Received 8 Mar 2010; revised 5 May 2010; accepted 5 May 2010; published 24 May 2010

fabrication is based on preform drilling it assures more flexibility in shaping fiber geometry than the stack and draw approach. Fibers with symmetry other than hexagonal can be fabricated [16], including structures with concentric rings of holes [17], dual core mPOF [18,19], elliptical core mPOF [20], mPOF with elliptical holes in the cladding [21] and hollow core mPOF [22]. The possibility of fabrication of Bragg gratings and long period gratings in mPOF was also demonstrated and several sensing applications of such elements have been already studied [23,24].

To our knowledge, so far there are no reports in the literature on the sensing characteristics of birefringent mPOF. In this paper, we present the results of investigations of a highly birefringent dual-core mPOF and report on the polarimetric and intermodal sensitivity of this fiber to hydrostatic pressure, strain and temperature.

2. Investigated mPOF

The investigated mPOF was purchased from Kiriama Pty Ltd. of Sydney, Australia. A SEM image of the fiber cross-section is shown in Fig. 1. In the microstructured region of this fiber there are two very large holes and a tiny bridge of PMMA between them. This bridge is so narrow that it does not permit light propagation. As a result, the modes are localized at both ends of the bridge where its thickness is greater. The diameter of small holes in the microstructured cladding vary in the fiber cross section in the range of 2-6 μm, the large holes have elliptical shape with axes measuring 14 × 17.5 μm and the separation of the cores' centers is about 11μm. Both cores are single mode and possess high birefringence induced by lack of hexagonal symmetry in their surroundings. Numerical simulations show that higher order modes are strongly attenuated. The calculated loss for the first higher order mode is greater that 2 dB/cm In the measurements no higher order modes were observed for propagation lengths longer than 20cm.

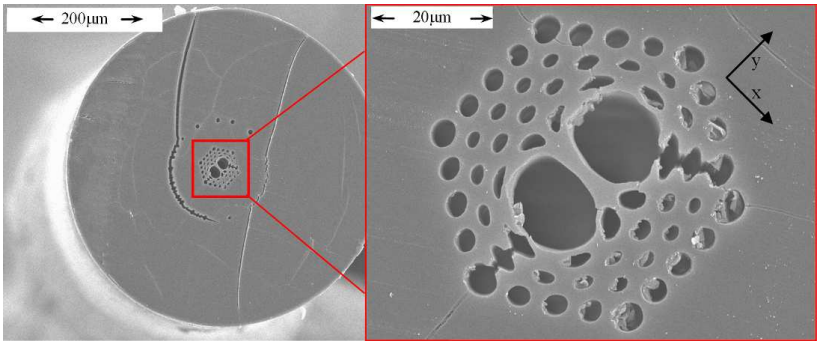

Fig. 1. SEM image of the investigated mPOF.

#125168 - $15.00 USD Received 8 Mar 2010; revised 5 May 2010; accepted 5 May 2010; published 24 May 2010

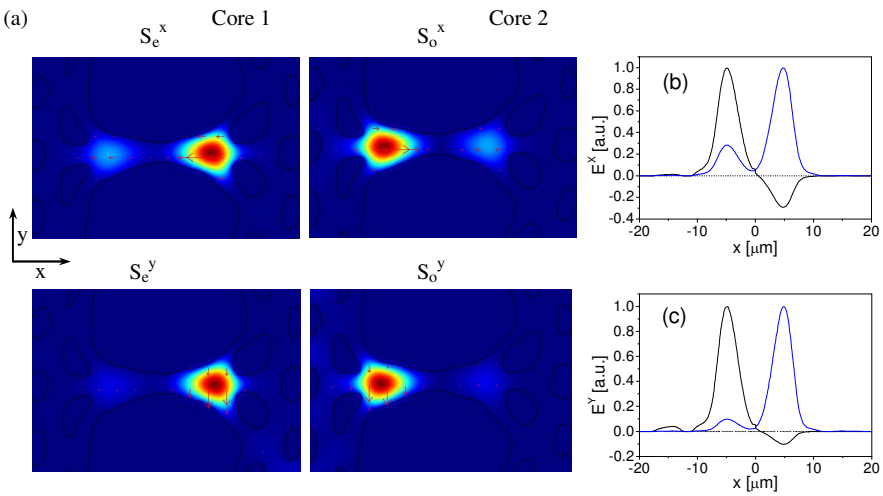

Fig. 2. Normalized maps of electric field distributions in all supermodes supported by the fiber (a) and cross-sections of field distributions in respective supermodes (b-c), λ = 560 nm.

Because of the short distance between the cores a coupling effect is observed. In such a case, light is guided in the form of orthogonally polarized even and odd supermodes spreading simultaneously over both cores. This effect was investigated previously in silica microstructured fibers [18,19,25]. In Fig. 2, we show the calculated amplitude distribution in quasi-symmetrical and quasi-antisymmetrical supermodes of orthogonal polarizations (respectively S_e^x, S_e^y, S_o^x, S_o^y) that can propagate in the investigated fiber. The amplitude distributions were calculated using finite element method (FEM), with the geometry of the fiber cross section obtained from the SEM image. The results of numerical simulations suggest that a relatively small fraction of the supermode power is confined in the non-excited core.

When a light beam is focused by a microscope objective on one core only, both quasi-symmetrical and quasi-antisymmetrical supermodes are excited at the fiber input. They propagate along the fiber with different velocities thus giving rise to energy transfer between the cores. The coupling strength is determined by the power division between the cores in the supermodes. When the power of the supermode is confined mostly in one core, the effect of coupling is weak. More equal distribution of power between the cores results in stronger coupling.

The coupling effect is clearly visible in the investigated fiber. In Fig. 3, we present spectrograms obtained by collecting the light from the excited core on the slit of a miniature spectrometer. The spectrograms were registered for x- and y-polarization of light at the fiber input. The contrast of interference fringes in the registered spectrogram is about 0.6, which corresponds to power division between dominant and weak supermodes in the ratio of about 90:10. Certain variations in contrast of a random character present in the registered spectrograms are caused by unwanted coupling between the supermodes guided in the fiber cores and the cladding modes originating in the microstructured region because of its lack of periodicity. The spacing between successive interference fringes is lower for the y-polarization, thus showing that the difference of group refractive indices for y-polarized supermodes is greater than for x-polarized supermodes. The estimated power division between the supermodes confined in the excited core, leads to the conclusion that relatively weak coupling takes place in the investigated fiber. This is also in agreement with the results of numerical simulations obtained for the actual fiber geometry, Fig. 2.

Finally, we have observed a very high impact of the fiber bending on the coupling effect. Therefore, in all measurements reported in this paper, care was taken not to bend the fiber when the applied measurand was changed. In particular, the spectrograms shown in Fig. 3 were registered for straight fiber.

#125168 - $15.00 USD Received 8 Mar 2010; revised 5 May 2010; accepted 5 May 2010; published 24 May 2010

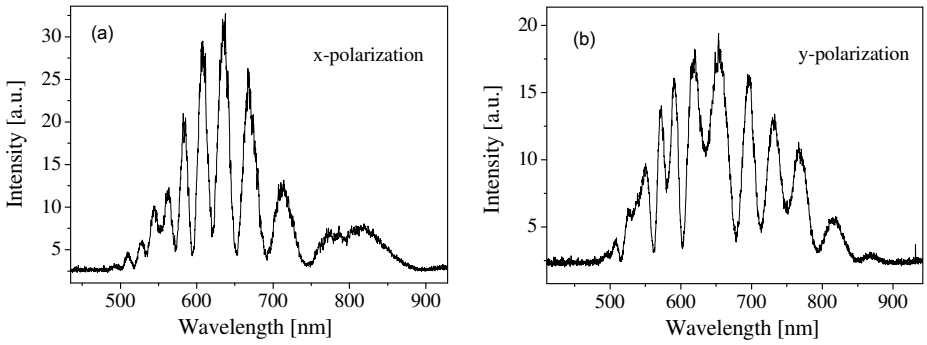

Fig. 3. Spectrograms registered at the output of the core 1 arising because of interference between the supermodes S_e^x, S_o^x (a) and S_e^y, S_o^y (b). The spectrograms were registered for straight fiber of length L = 0.362 m, core 1 was excited at the fiber input with x- and y-polarized light, respectively.

3. Measurements of phase and group modal birefringence

Measurements of group modal birefringence and polarimetric sensitivities were carried out individually in both cores using a spectral interferometric method [4]. The measurement set-up consisted of a broad band light source (supercontinuum), polarizer and analyzer placed at the ends of the tested fiber and aligned at 45° to its polarization axes, see Fig. 4. Such alignment causes pairs of orthogonally polarized supermodes to be excited in the fiber which interfere at its output after passing through the analyzer. A microscope objective formed a sharp image of the fiber end-face on the entrance slit of the spectrometer. In this way, we could register spectral interference fringes individually for each core. Due to interference between polarization supermodes of the same symmetry, the outgoing spectrum is modulated by high frequency interference fringes superimposed on low frequency fringes caused by intermodal interference of supermodes of the same polarization, Fig. 5. When the light polarized at 45° to the fiber symmetry axis is focused on core 1, we excite the dominant pair of supermodes S_e^x, S_e^y confined mostly in this core and also weaker supermodes S_o^x, S_o^y confined predominantly in core 2. As a result, the polarization interference fringes observed in core 1 are related to the interference of the dominating supermodes S_e^x, $S_e^{y.}$. They have a very good contrast, which is only slightly perturbed by interference between the odd supermodes S_o^x, S_o^y mostly confined in the core 2 or by coupling to the cladding modes, see Fig. 5.

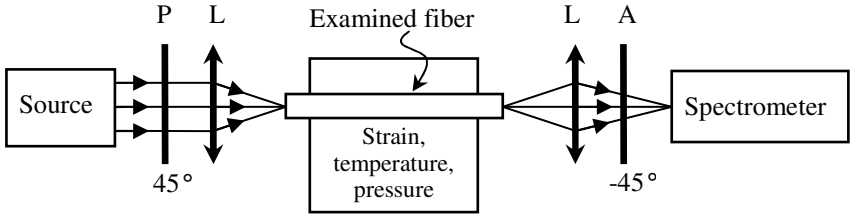

Fig. 4. Setup for measurements of birefringence and polarimetric sensitivity to different measurands in each core individually, P-polarizer, A-analyzer, L-microscope objective.

#125168 - $15.00 USD Received 8 Mar 2010; revised 5 May 2010; accepted 5 May 2010; published 24 May 2010

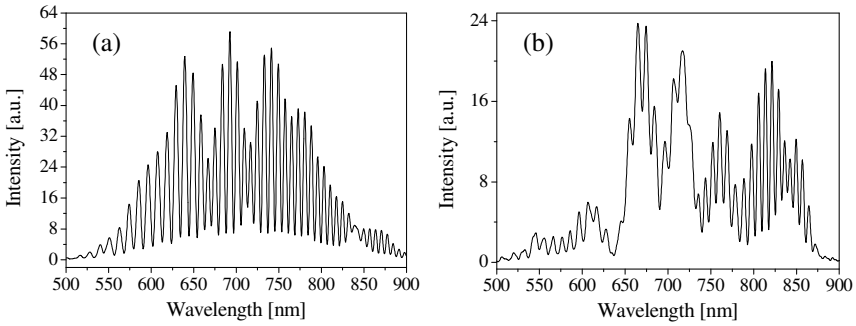

Fig. 5. Spectral fringes arising due to interference of orthogonally polarized supermodes at the output of core 1 (a) and core 2 (b) when core 1 is excited. The spectrograms were registered for straight fiber of length L = 0.258 m.

When the image of core 2 is focused on the entrance slit of the spectrometer, much more noisy interference fringes are observed. Clearly visible contrast fading of the polarization interference fringes in core 2 is related to the superposition of two interference signals (having slightly different spatial frequency) produced by pairs of polarization supermodes S_e^x, S_e^y and S_o^x, $S_o^{y.}$, which in the non excited core have similar amplitudes. An analogous effect is observed when core 2 is purely excited at the fiber input. In this case, dominating S_o^x, S_o^y supermodes contributes mostly to the interference signal collected at the output of core 2. These observations lead us to the conclusion that because of the relatively weak coupling effect, we can measure birefringence and sensitivity in each core individually. In particular, to measure birefringence in core 1, we must purely excite and detect the interference signal at the output of this core. A similar procedure was applied to measure birefringence and sensitivity in core 2.

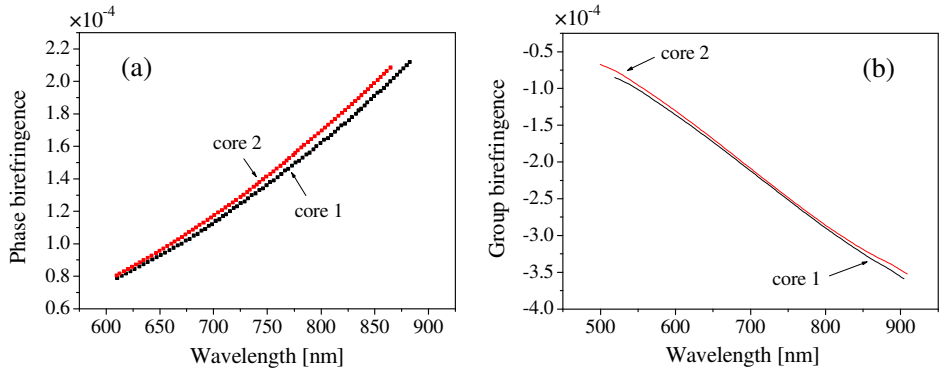

Fig. 6. Results of measurements of phase modal birefringence (a) and group modal birefringence (b) in the two cores.

To determine the spectral dependence of the phase modal birefringence B from the registered spectrograms, we first measured, using the lateral force method [26], the beat length defined as:

$$L_B = \lambda / B. \qquad (1)$$

The obtained values at λ = 610 nm were 7.75 mm and 7.61 mm, respectively, for the first and the second core. Using Eq. (1), we calculated the phase modal birefringence B at λ = 610 nm and the absolute value of the phase shift between polarization modes at this wavelength.

#125168 - $15.00 USD Received 8 Mar 2010; revised 5 May 2010; accepted 5 May 2010; published 24 May 2010

When the absolute interference order is known at one wavelength, it is possible to determine the phase shift at each intensity extreme in the registered spectrograms and finally to calculate the spectral dependence of the phase modal birefringence using the following relation:

$$B(\lambda) = \frac{\Delta\phi(\lambda)\lambda}{2\pi L}. \tag{2}$$

The group modal birefringence was determined for both cores from the following relation:

$$G(\lambda) = -\frac{\lambda^2}{2\pi L}\frac{d(\Delta\phi(\lambda))}{d\lambda}. \tag{3}$$

To carry out the differentiation in the above equation, the dependence $\Delta\varphi(\lambda)$ was approximated with a 6th degree polynomial. The results of measurements of B and G are presented in Fig. 6. Birefringence in both cores strongly increases with wavelength and significantly exceeds 10^{-4} in the visible range. This is a typical behavior of B and G for microstructured fibers with purely geometrical birefringence. Because both cores have similar shapes and sizes, the measured values of B and G differ only a little between the cores (a maximum of 10%).

4. Measurements of the polarimetric sensitivity to hydrostatic pressure, strain and temperature

The polarimetric sensitivity of the fiber to a specific parameter, X, represents the phase difference between polarization modes induced by unit change of the parameter over unit length of the fiber and can be expressed in the following way:

$$K_X = \frac{1}{L_X}\frac{d(\phi_x - \phi_y)}{dX} = \frac{2\pi}{\lambda}\left[\frac{\partial B}{\partial X} + \frac{B}{L_X}\frac{\partial L_X}{\partial X}\right]. \tag{4}$$

An interferometric system used to measure the sensitivity to hydrostatic pressure and elongation is shown in Fig. 4. A microscope objective formed a sharp image of the fiber endface on the entrance slit of the spectrometer. In this way, we could register spectral interference fringes for different values of applied measurand individually for each core thus making it possible to measure the polarimetric sensitivity for each core. To measure sensitivity in core 1, we introduced into this core a light beam polarized at 45° to the fiber symmetry axes and monitored the spectral interference signal at the output of this core. For such excitations S_e^x, S_e^y supermodes contribute primarily to the interference signal. A similar procedure was applied to measure the sensitivity in core 2, in which the supermodes S_o^x, S_o^y are predominantly confined. By aligning the input polarizer in parallel to one of the fiber symmetry axes, we could also selectively excite the supermodes of the same polarization and measure the intermodal phase sensitivity named by $K_X^{\text{int}-x}$ and $K_X^{\text{int}-y}$, respectively for pairs of supermodes of x- and y-polarization.

To determine the K_X, the shift of spectral interference fringes was recorded as a function of applied measurand, Fig. 7. By registering the displacement of interference minima $\lambda_{\min}(X)$ versus measurand change, we determined the polarimetric sensitivity from the following relation:

$$K_X = -\frac{2\pi}{L_X}\frac{d}{dX}\left(\frac{\lambda_{\min}(X)}{\Delta\lambda}\right), \tag{5}$$

where $\Delta\lambda$ is the fringe spacing and L_X is the length of the fiber exposed to measurand change. One should note that displacement of the interference fringes towards shorter wavelength induced by increasing measurand corresponds to a positive sign of K_X.

#125168 - $15.00 USD Received 8 Mar 2010; revised 5 May 2010; accepted 5 May 2010; published 24 May 2010

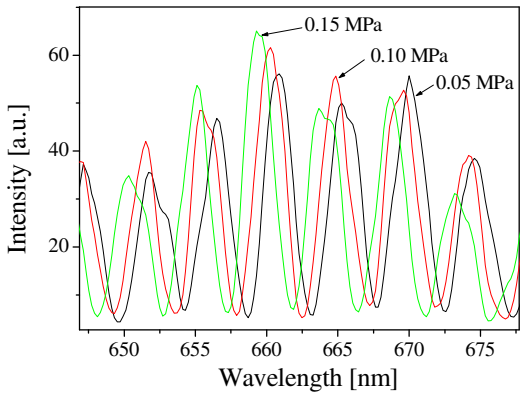

Fig. 7. Displacement of spectral interference fringes induced by increasing hydrostatic pressure. Length of the fiber exposed to pressure changes is L_P = 0.362 m, total fiber length is L = 0.66 m, spectrogram registered for core 1.

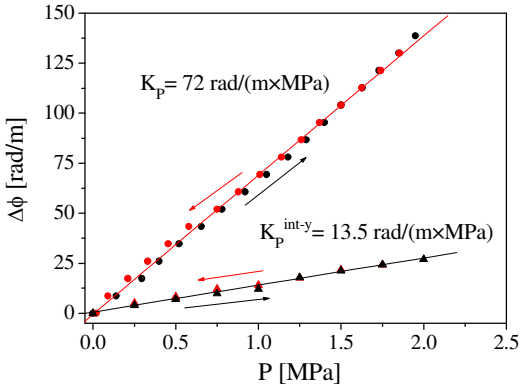

Fig. 8. Phase shift between polarization supermodes (K_P) and supermodes of y-polarization (K_P^{int-y}) induced by increasing and decreasing hydrostatic pressure. Measurements were carried out for core 1, λ = 710 nm. Length of the fiber exposed to pressure changes is L_P = 0.362 m, total fiber length is L = 0.66 m.

In measurements of the pressure sensitivity, the tested fiber was installed in a specially designed oil chamber and subjected to pressure changes in the range from 0 to 2 MPa. The results of measurements of the polarimetric sensitivity K_P in core 1 are presented in Fig. 8. The fiber shows a repeatable response to hydrostatic pressure with small hysteresis in the investigated pressure range up to 2 MPa (20 bars) and relatively high polarimetric sensitivity up to K_P = 72 rad/(MPa × m) at λ = 710 nm. The polarimetric sensitivity measured for core 2 is only 5% greater than that of core 1. In Fig. 8, we also present the effect of hydrostatic pressure on the interference of the supermodes of y-polarization. An increase of the phase shift between the supermodes is observed in response to applied pressure, with the rate of about K_P^{int-y} = 13.5 rad/(MPa × m). The value of K_P^{int-x} is the same within the measurement precision of about 3%.

The measured polarimetric sensitivity K_P has a positive sign, which means that birefringence increases in response to applied pressure. In the case of hydrostatic pressure, the last term in Eq. (4), representing the pressure-induced fiber elongation is small and therefore it

#125168 - $15.00 USD Received 8 Mar 2010; revised 5 May 2010; accepted 5 May 2010; published 24 May 2010

can be disregarded. Based on this assumption, we determined the sensitivity of the phase modal birefringence to pressure from the following relation:

$$\frac{dB}{dp} = \frac{\lambda K_X}{2\pi}. \tag{6}$$

As shown in Fig. 9, the sensitivity dB/dp is almost wavelength independent, while K_P strongly decreases against wavelength following a $1/\lambda$ function. The measurement results were compared with numerical simulations of the polarimetric sensitivity to pressure carried out in the same way as done recently for microstructured silica fiber [27]. According to this analysis, as is the case in silica fibers, the sensitivity dB/dp in mPOF is mostly associated with the material birefringence induced in the core region by applied pressure. This explains the weak wavelength dependence of dB/dP both in silica and polymer microstructured fibers. As reported in our earlier publication [27], the K_P in silica PCFs has a negative sign, however its absolute value is close to the sensitivity of the investigated mPOF. For example, the K_P reported in [27,28] for the birefringent microstructured silica fibers ranges from −14.8 rad/MPa × m up to −100 rad/MPa × m (at 830 nm) depending on the fiber construction. The different signs of K_P in silica and PMMA microstructured fibers is related to different signs of the stress-optic coefficients in these two materials, which are equal to $\Delta C_{SiO2} = 3.52 \times 10^{-12}$ Pa^{-1} [29] and $\Delta C_{PMMA} = -2.31 \times 10^{-12}$ Pa^{-1} [30], respectively.

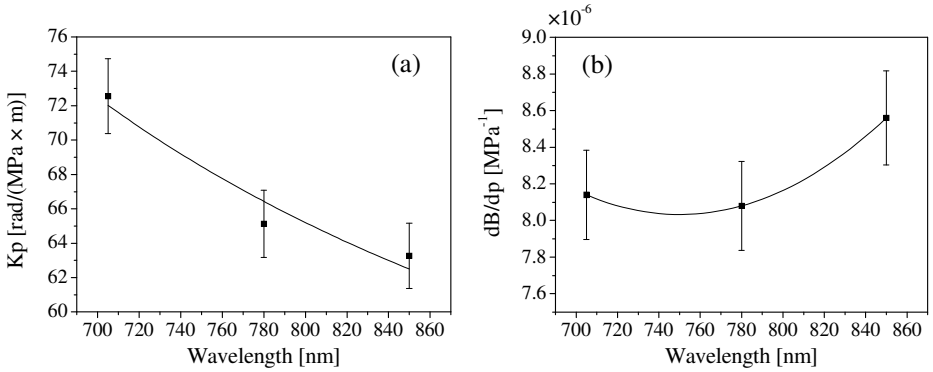

Fig. 9. Spectral dependence of the polarimetric sensitivity to hydrostatic pressure K_p (a) and sensitivity of modal birefringence to hydrostatic pressure *dB/dp* (b)

To measure sensitivity to strain, a fiber of length $L_\varepsilon = 0.662$ m was attached with epoxy glue to two mechanical stages and stretched up to 8 mstrain. The measurements were conducted in the same way as for hydrostatic pressure. The interference fringes clearly shift towards short wavelengths for increasing strain, which indicates that the sensitivity K_ε has a positive sign. The results of measurements of K_ε at $\lambda = 710$ nm are presented in Fig. 10.

#125168 - $15.00 USD Received 8 Mar 2010; revised 5 May 2010; accepted 5 May 2010; published 24 May 2010

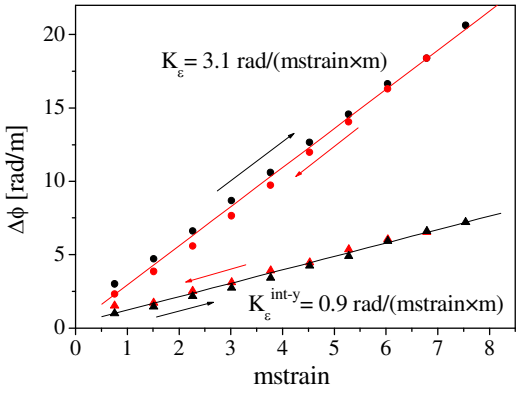

Fig. 10. Phase shift between polarization supermodes (K_ε) and supermodes of y-polarization (K_ε^{int-y}) induced by increasing and decreasing strain, λ = 710 nm. Length of the fiber subjected to elongation is L_{strain} = 0.662 m, total fiber length is L = 0.78 m, measurement carried out for core 1.

The investigated fiber shows repeatable response to elongation with small hysteresis and medium polarimetric sensitivity K_ε = 3.1 rad/(mstrain × m). The sensitivity in core 2 is only about 4% greater than in core 1. In Fig. 10, we also show the effect of strain on interference of the supermodes of y-polarization propagating in the two cores. The phase shift between the supermodes changes linearly against applied strain with the rate of about K_ε^{int-y} = 0.9 rad/(mstrain × m). The value of K_ε^{int-x} is only about 3% lower than K_ε^{int-y}.

The strain sensitivity of the investigated PMMA fiber K_ε = 3.1 rad/(m × mstrain) is small compared to conventional birefringent silica fibers such as Bow-Tie (K_ε = 18 rad/m × mstrain) or elliptical core fiber (K_ε = –5 rad/m × mε) [31,32]. It is worth mentioning that the measured sensitivity K_ε is almost the same as the sensitivity of the birefringent microstructured silica fiber reported in [4] (K_ε = -2.8 rad/m × mε) except that the signs of K_ε in the PMMA and silica fibers are opposite.

There are three physical factors responsible for the strain-induced phase shift between the polarization modes in the investigated fiber. The first one is related to fiber elongation and is represented by the second term in Eq. (4). Its contribution to K_ε always has a positive sign. The second effect is connected to diminishing the fiber radial dimensions with the rate of νε, where ν is Poisson's ratio and ε is the applied strain, which in case of microstructured fibers results in an increase of the phase modal birefringence. Because of significant difference between the Poisson ratio of silica and PMMA, ν_{SiO2} = 0.16 [29] and ν_{PMMA} = 0.35 [30], the strain-induced increase in modal birefringence is much greater in PMMA microstructured fibers than in silica fibers of the same geometry. Finally, the refractive index of PMMA is diminished due to elongation, which can increase or decrease its modal birefringence, depending on the fiber geometry. It is difficult to intuitively evaluate the simultaneous impact of those three effects on polarimetric sensitivity to strain and, therefore, more detailed theoretical analysis is required to explain the different signs of K_ε in PMMA and silica fibers.

#125168 - $15.00 USD Received 8 Mar 2010; revised 5 May 2010; accepted 5 May 2010; published 24 May 2010

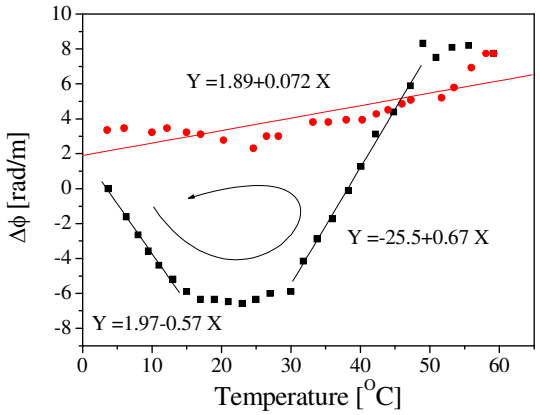

Fig. 11. Phase shift between polarization supermodes induced by increasing and decreasing temperature measured for annealed fiber at λ = 710 nm. The length of the fiber subjected to temperature changes is L_T = 0.22 m, total fiber length is L = 0.78 m, measurement carried out for core 1.

Measurement of the polarimetric sensitivity to temperature was conducted for several pieces of the investigated fiber in the temperature range of 3-60°C. Depending on the thermal history of the specific piece of the fiber, we observed very different polarimetric responses to temperature, typically with high nonlinearity and hysteresis. The fiber sensitivity K_T averaged over the full temperature span changes from −1 rad/K × m to 1 rad/K × m depending on the temperature cycle. The origin of such high differences in K_T between successive temperature cycles is not clear. Perhaps they are caused by release of frozen-in stress at increased temperatures. In Fig. 11, we present the temperature response of a fiber that was annealed for 20 h at a temperature of 100°C. We observed that annealing improves repeatability and decreases the amplitude of the temperature response, however, nonlinearity and hysteresis is still observed. For annealed fiber the local temperature coefficients change from −0.6 rad/K × m to 0.7 rad/K × m.

5. Conclusions

To our knowledge, we report for the first time on the sensing characteristics of highly birefringent microstructured polymer fiber. The investigated fiber possesses two cores, with high birefringence in each core exceeding 10^{-4} in the visible range and shows a spectral dependence of B and G typical for geometrical birefringence. Because of small coupling between the cores, we could characterize each core individually. Small differences between the cores (of the order of a few %) were observed for all investigated parameters, including phase and group modal birefringence as well as polarimetric sensitivities. This is related to the relatively high symmetry of the investigated fibers, as a result of the cores having similar shapes and sizes.

Two large holes in the microstructured region of the investigated fiber are responsible for its high polarimetric sensitivity to hydrostatic pressure, reaching K_P = 72 rad/(MPa × m) at λ = 710 nm. Moreover, the response to pressure is linear and shows small hysteresis in the investigated pressure range of 20 bars. The difference in sign of K_P in the investigated fiber and in silica microstructured fibers of similar geometry is related to the different signs of the stress-optic coefficients in the two materials.

The fiber shows repeatable response to strain with small hysteresis in the strain range up to 8 mstrain. The measured polarimetric sensitivity K_ε = 3.1 rad/(mstrain × m) at λ = 710 nm in the investigated fiber is similar in absolute value but different in sign compared to silica microstructured fibers of the same geometry [4]. This is most probably caused by the much

#125168 - $15.00 USD Received 8 Mar 2010; revised 5 May 2010; accepted 5 May 2010; published 24 May 2010

greater Poisson's ration of PMMA compared to silica. Finally, we have also measured the intermodal phase sensitivity to hydrostatic pressure and strain. These parameters are much lower than corresponding polarimetric sensitivities and equal K_P^{int} = 13.5 rad/(MPa × m) and $K_\varepsilon^{\text{int}}$ = 0.9 rad/(mstrain × m).

Acknowledgements

The work described in this paper was partially carried out with the support of the Photonic Skins for Optical Sensing project (PHOSFOS), a small/medium-scale focused project funded by the European Commission through the 7th ICT-Framework Programme and the Statutory Grant at Wroclaw University of Technology. M. K. Szczurowski, G. Satkiewicz-Barabach and W. Urbanczyk acknowledge support of the FNP Program MISTRZ.

#125168 - $15.00 USD Received 8 Mar 2010; revised 5 May 2010; accepted 5 May 2010; published 24 May 2010